Earth and Planetary Science Letters, 53 (1981) 69–83
Elsevier Scientific Publishing Company, Amsterdam – Printed in The Netherlands

[4]

SPHERICAL EARTH GRAVITY AND MAGNETIC ANOMALY ANALYSIS BY EQUIVALENT POINT SOURCE INVERSION

RALPH R.B. VON FRESE, WILLIAM J. HINZE and LAWRENCE W. BRAILE

Department of Geosciences, Purdue University, West Lafayette, IN 47907 (U.S.A.)

Received June 11, 1980
Revised version received December 2, 1980

To facilitate geologic interpretation of satellite elevation potential field data, analysis techniques are developed and verified in the spherical domain that are commensurate with conventional flat earth methods of potential field interpretation. A powerful approach to the spherical earth problem relates potential field anomalies to a distribution of equivalent point sources by least squares matrix inversion. Linear transformations of the equivalent source field lead to corresponding geoidal anomalies, pseudo-anomalies, vector anomaly components, spatial derivatives, continuations, and differential magnetic pole reductions. A number of examples using 1°-averaged surface free-air gravity anomalies and POGO satellite magnetometer data for the United States, Mexico and Central America illustrate the capabilities of the method.

1. Introduction

Regional-scale anomalies of the earth's magnetic and gravity fields provide important constraints for refining the basic model of plate tectonics and understanding intra-plate dynamics. These anomalies, especially when combined with other geophysical and geological data, may be anticipated to yield much information concerning regional physical property variations that are important for determining the structure, dynamics and geological history of the earth's crust and upper mantle. The realization of the importance of these observations has led to increased availability of highly accurate regional-scale potential field data for analysis. Commensurate advances in data analysis for lithospheric interpretation, however, have not kept pace and generally are unavailable.

Regional gravity and magnetic surveys represent spherically composited data for areas ranging in size from a few degrees to complete global coverage by satellite measurements. Typical processing objectives include data regridding, continuation, differentiation, and other wavelength filtering operations. For regional magnetic surveys it also is desirable from the standpoint of lithospheric interpretation to reduce the data for the variable geomagnetic field effects of inclination, declination and intensity.

Spherical surface harmonic functions are a natural representation for spherically registered gravity and magnetic anomaly fields. In general, spherical harmonics also are well suited for accomplishing the processing objectives described above because these operations involve only modifications of the geometric variables of the anomalies. However, the problem of representing potential field measurements over a spherical domain with an orthonormal set of spherical harmonic functions in general is a formidable task of computation (e.g. [1]), especially when it is desired to retain for analysis higher-order and -degree terms involving wavelengths of the order of a few hundred kilometers or less.

When potential field anomalies are spherically registered at constant elevation, Fourier transform methods yield a simpler numerical representation of the data which is suitable for strike-sensitive and wavelength filtering. These filters are applicable because the frequency response of the potential field anomaly is invariant for any uniform orthogonal

0012-821X/81/0000–0000/$02.50

translation of the degree coordinates of the anomaly over the spherical domain. As an example, low-pass filtering a set of 1°-averaged free-air gravity anomalies can be useful to help eliminate topographic mass contributions, where it is noted that topographic mass effects tend to be minimized when free-air gravity anomalies are averaged over areas of the order 3° and larger [2,3].

Fourier transform methods applied in the spherical domain to discriminate anomaly source characteristics, however, normally necessitate regridding of the data to a Cartesian plane. The regridding procedure with all its attendant problems is required in such cases because the Fourier frequency characterization of an anomaly is variant for spherical translations of the anomaly source. Continuation and differentiation by Fourier transform methods also require Cartesian reregistration of the data to avoid distortions due to a Nyguist degree-wavelength which is variable in terms of the linear radial dimension of these operations.

Another approach to spherical earth processing is to invert potential field anomalies on a spherical distribution of equivalent point sources. In contrast to processing by spherical harmonics or Fourier transform methods, equivalent point source inversion yields numerically efficient representations of potential field anomalies to any desired degree of wavelength resolution which can be directly processed in the spherical domain.

In principle, equivalent point source inversion takes advantage of the ambiguity of source physical properties and distributions which is a feature inherent to all potential field anomalies. Every potential field observation, for example, represents the integrated effect of sources which may be characterized with equal facility by an infinite number of combinations of source physical properties and geometric parameters (e.g. [4,5]). The objective, then, is to relate a set of spherically registered potential field measurements to a distribution of equivalent sources with numerical properties which are amenable to spherical earth processing objectives.

Especially convenient from a numerical standpoint are equivalent point sources because the characteristics of their gravity and magnetic potentials are simplest to describe mathematically. As will be demonstrated, the point source potential and all its geophysically interesting derivatives can always be expressed as the product of an appropriate physical property value and a purely geometrical point source function which describes the inverse distance between source and observation points. By specifying the geometrical distribution of the equivalent point sources, the problem reduces to one of determining a set of physical property values by matrix inversion techniques such that the potential field anomalies due to the equivalent point source distribution approximate the observed anomalies to a specified precision. Once a suitable set of physical property values has been found, the equivalent source field representation of the observed anomalies is calculated by summing at each observation point the anomaly effect due to each of the equivalent point sources. Hence, to obtain an equivalent source field representation of the continuation, differentiation, etc, of the observed anomalies to the precision reflected in the original approximation, the summation procedure is simply repeated using the appropriate geometrical point source function.

Potential field analyses in the past have employed a variety of surrogate sources including Cartesian distributions of point masses [6] and lines of magnetic dipoles [7] as well as spherical magnetic prism distributions [8]. In this discussion, equivalent point sources are used to develop a systematic procedure for comprehensive geologic analysis of both gravity and magnetic anomalies in spherical coordinates. To illustrate the mechanism and versatility of the procedure, it is desirable to describe explicitly the properties of gravity point poles and magnetic point dipoles which facilitate potential anomaly field analyses in the spherical domain that are commensurate with conventional flat earth methods of potential field interpretation.

2. The gravity point pole potential

The gravity point pole is defined as a mass of negligible diameter when compared to the distance between the mass source and observation points. Its scalar gravitational potential $GP(R)$ at a point with spherical coordinates (r, θ, ϕ) located a distance $\vec{R}$ from the source point (r_1, θ_1, ϕ_1) is given by:

$$GP(R) = \frac{G * \Delta m}{|\vec{r} - \vec{r}_1|} = \frac{G * \Delta m}{R} \qquad (1)$$

where G = universal gravitational constant (= 6.67 X 10^{-8} cm^3 g^{-1} s^{-2}), Δm = mass contrast of the point pole,

$$R = |\vec{r} - \vec{r}_1| = (r^2 + r_1^2 - 2rr_1 \cos\delta)^{1/2}\,, \qquad (2)$$

$\vec{r}$ = radius vector directed from observation point (r, θ, ϕ) to earth's center, $\vec{r}_1$ = radius vector directed from source point (r_1, θ_1, ϕ_1) to earth's center, δ = angle between $\vec{r}$ and $\vec{r}_1$ at the earth's center, such that:

$$\cos\delta = \cos\theta\cos\theta_1 + \sin\theta\sin\theta_1\cos(\phi - \phi_1)\,,$$

θ, θ_1 = co-latitude coordinates of observation and source points, respectively, and ϕ, ϕ_1 = longitude coordinates of observation and source points, respectively.

The geometric characteristics of the point source potential are illustrated in Fig. 1.

Because of the dependence of the potential on the inverse of the distance $\vec{R}$, the derivatives of the point pole potential $GP(R)$ are linearly related by the relationship:

$$\frac{\partial^n}{\partial R^n}\left(\frac{1}{R^k}\right) = \frac{(-1)^n}{R^{k+n}} * \frac{(k+n-1)!}{(k-1)!} \qquad (3)$$

This result provides a useful function for considering derivatives of the potential.

Now, the vector gravitational force field $GF(\vec{R})$ at the distance $\vec{R}$ is given in spherical coordinates by the negative gradient of the scalar point pole potential as:

$$GF(\vec{R}) = -\vec{\nabla}\{GP(R)\}$$

$$= \frac{-\partial}{\partial R}\{GP(R)\}\,\vec{\nabla}R = \left\{-G\,\frac{\partial}{\partial R}\left(\frac{1}{R}\right)\vec{\nabla}R\right\}\Delta m$$

where the gradient of R is:

$$\vec{\nabla}R = \frac{\partial R}{\partial r}\hat{e}_r + \frac{1}{r}\frac{\partial R}{\partial\theta}\hat{e}_\theta + \frac{1}{r\sin\theta}\frac{\partial R}{\partial\phi}\hat{e}_\phi$$

such that:

$$\frac{\partial R}{\partial r} = \frac{r - r_1\cos\delta}{R} = \frac{A}{R}\,, \qquad (4)$$

$$\frac{1}{r}\frac{\partial R}{\partial\theta} = \frac{r_1\{\sin\theta\cos\theta_1 - \cos\theta\sin\theta_1\cos(\phi - \phi_1)\}}{R}$$

$$= \frac{B}{R} \qquad (5)$$

$$\frac{1}{r\sin\theta}\frac{\partial R}{\partial\phi} = \frac{r_1\sin\theta_1\sin(\phi - \phi_1)}{R} = \frac{C}{R}\,, \qquad (6)$$

and $\hat{e}_r$, $\hat{e}_\theta$ and $\hat{e}_\phi$ are the spherically orthogonal basis vectors. Accordingly, the gravitational force field at (r, θ, ϕ) is given by:

$$GF(\vec{R}) = \left\{-G\,\frac{\partial}{\partial R}\left(\frac{1}{R}\right) * \left(\frac{A}{R}\hat{e}_r + \frac{B}{R}\hat{e}_\theta + \frac{C}{R}\hat{e}_\phi\right)\right\}\Delta m\,, \qquad (7)$$

where the radial scalar component is:

$$\Delta g = \left\{-G\,\frac{\partial}{\partial R}\left(\frac{1}{R}\right) * \frac{\partial R}{\partial r}\right\}\Delta m = \left\{\frac{G * A}{R^3}\right\}\Delta m\,, \qquad (8)$$

the horizontal θ-co-latitude scalar component is:

$$\left\{-G\,\frac{\partial}{\partial R}\left(\frac{1}{R}\right) * \left(\frac{1}{r}\frac{\partial R}{\partial\theta}\right)\right\}\Delta m = \left\{\frac{G * B}{R^3}\right\}\Delta m\,, \qquad (9)$$

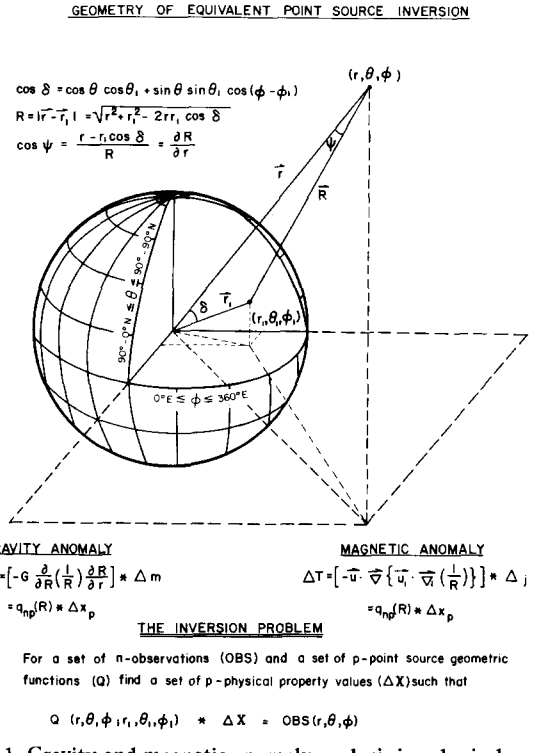

Fig. 1. Gravity and magnetic anomaly analysis in spherical coordinates by equivalent point source inversion (see text for details).

and the horizontal ϕ-longitude scalar component is:

$$\left\{-G\frac{\partial}{\partial R}\left(\frac{1}{R}\right) * \left(\frac{1}{r\sin\theta}\frac{\partial R}{\partial \phi}\right)\right\}\Delta m = \left\{\frac{G * C}{R^3}\right\}\Delta m \tag{10}$$

Also, because:

$$\left\{\frac{\partial GP(R)}{\partial R}\right\}^2 = \left\{\frac{\partial GP(R)}{\partial R}\right\}^2 * \left\{\left(\frac{\partial R}{\partial r}\right)^2 + \left(\frac{1}{r}\frac{\partial R}{\partial \theta}\right)^2 + \left(\frac{1}{r\sin\theta}\frac{\partial R}{\partial \phi}\right)^2\right\},$$

the total horizontal component of the gravitational force field (7) can be expressed in terms of the radial component (8) as:

$$\frac{\partial GP(R)}{\partial R}\left\{\left(\frac{1}{r}\frac{\partial R}{\partial \theta}\right)^2 + \left(\frac{1}{r\sin\theta}\frac{\partial R}{\partial \phi}\right)^2\right\}^{1/2} = \Delta g\left\{\left(\frac{R}{A}\right)^2 - 1\right\}^{1/2} \tag{11}$$

In relating a set of gravity observations to equation (7), it is important to recognize the distinction between the total gravity anomaly and the gravity effect due to local geologic mass variations. In geophysical practice, the quantity which is considered is the anomalous perturbation of the radial component of the earth's geocentric gravitational field. The use of this quantity, which commonly is called the gravity effect, Δg, for lithospheric analysis assumes the gravity anomaly due to geological mass variations is so small that perturbations of the earth's gravity field in any direction other than the normal are negligible. Thus, when relating an observed gravity anomaly value to the gravitational force field of a point pole, the objective is to express the observed gravity effect as the radial component of equation (7) which is given by equation (8).

For lithospheric interpretation, it frequently is desirable to analyze the spatial derivatives of the gravity anomalies. Differentiation of a set of regional-scale gravity observations, for example, can help identify the higher-frequency crustal components of the anomaly field. The derivatives also provide useful information for modeling the geometric characteristics of anomalous sources.

To obtain equivalent source field representations of the spatial derivatives for a set of gravity observations it is necessary to develop the spatial derivatives of the gravity effect of the gravity point pole. The first-order derivative components of the point pole gravity effect can be calculated from the negative gradient as:

$$\begin{aligned}-\vec{\nabla}(\Delta g) &= -G\left\{\vec{\nabla}\left(\frac{A}{R^3}\right)\right\}\Delta m \\ &= -G\left\{A\vec{\nabla}\left(\frac{1}{R^3}\right) + \left(\frac{1}{R^3}\right)\vec{\nabla}A\right\}\Delta m \\ &= \left[-G\left\{A\frac{\partial}{\partial R}\left(\frac{1}{R^3}\right) + \left(\frac{1}{R^3}\right)\frac{\partial A}{\partial R}\right\}\vec{\nabla}R\right]\Delta m\end{aligned} \tag{12}$$

where the components of $\vec{\nabla}R$ are given by equations (4), (5) and (6). Now, to evaluate $(\partial A/\partial R)$ note that $(\partial A/\partial r) = (\partial A/\partial R)(\partial R/\partial r) = 1$ and, hence:

$$(\partial A/\partial R) = R/A \tag{13}$$

Accordingly, equation (12) becomes:

$$-\vec{\nabla}(\Delta g) = \left\{-G\left(\frac{1}{R^2A} - \frac{3A}{R^4}\right) * \left(\frac{A}{R}\hat{e}_r + \frac{B}{R}\hat{e}_\theta + \frac{C}{R}\hat{e}_\phi\right)\right\}\Delta m$$

where the scalar first radial derivative of Δg is given by:

$$\frac{-\partial \Delta g}{\partial r} = \left\{-G\left(\frac{1}{R^3} - \frac{3A^2}{R^5}\right)\right\}\Delta m \tag{14}$$

the scalar first horizontal θ-co-latitude derivative of Δg is derived from:

$$-\frac{1}{r}\frac{\partial \Delta g}{\partial \theta} = \left\{-G\left(\frac{B}{R^3A} - \frac{3AB}{R^5}\right)\right\}\Delta m \tag{15}$$

and the first horizontal ϕ-longitudinal derivative of Δg is obtained from:

$$\frac{-1}{r\sin\theta}\frac{\partial \Delta g}{\partial \phi} = \left\{-G\left(\frac{C}{R^3A} - \frac{3AC}{R^5}\right)\right\}\Delta m \tag{16}$$

Also, by the same argument which led to the development of equation (11) it can be shown that the total horizontal gradient of Δg may be expressed in terms of its radial derivative according to the relation:

$$\frac{\partial \Delta g}{\partial R}\left\{\left(\frac{1}{r}\frac{\partial R}{\partial \theta}\right)^2 + \left(\frac{1}{r\sin\theta}\frac{\partial R}{\partial \phi}\right)^2\right\}^{1/2}$$

$$= \frac{\partial \Delta g}{\partial r}\left\{\left(\frac{R}{A}\right)^2 - 1\right\}^{1/2} \qquad (17)$$

Another useful tool for lithospheric interpretation is the Laplacian which, in terms of the gravity effect of the point pole, is given by:

$$\nabla^2(\Delta g) = \frac{1}{r^2}\frac{\partial}{\partial r}\left(r^2 \frac{\partial \Delta g}{\partial r}\right) + \frac{1}{r^2 \sin\theta}\frac{\partial}{\partial \theta}\left(\sin\theta \frac{\partial \Delta g}{\partial \theta}\right) + \frac{1}{r^2 \sin^2\theta}\frac{\partial^2 \Delta g}{\partial \phi^2}$$

$$= \left\{\frac{\partial^2 \Delta g}{\partial r^2} + \frac{2}{r}\frac{\partial \Delta g}{\partial r}\right\} + \left\{\frac{1}{r^2}\frac{\partial^2 \Delta g}{\partial \theta^2} + \frac{1}{r^2}\cot\theta \frac{\partial \Delta g}{\partial \theta}\right\} + \left\{\frac{1}{r^2 \sin^2\theta}\frac{\partial^2 \Delta g}{\partial \phi^2}\right\}$$

Now, $\nabla^2(\Delta g) = 0$ because Δg is a potential function and, hence:

$$-\left\{\frac{\partial^2 \Delta g}{\partial r^2} + \frac{2}{r}\frac{\partial \Delta g}{\partial r}\right\} = \frac{1}{r^2}\left\{\frac{\partial^2 \Delta g}{\partial \theta^2} + \cot\theta \frac{\partial \Delta g}{\partial \theta} + \frac{1}{\sin^2\theta}\frac{\partial^2 \Delta g}{\partial \phi^2}\right\} \qquad (18)$$

where $(\partial \Delta g/\partial r)$ is evaluated in (14) and the second radial derivative is given by:

$$\frac{\partial^2 \Delta g}{\partial r^2} = \frac{\partial}{\partial R}\left\{\frac{\partial \Delta g}{\partial r}\right\}\frac{\partial R}{\partial r} = G\left\{\frac{15A^3}{R^7} - \frac{9A}{R^5}\right\}\Delta m \qquad (19)$$

Equation (18) relates the horizontal gravity anomaly curvature to the radial curvature which is the Laplacian component normally computed for analysis. Because of the dependence of the Laplacian on first- and second-order derivatives it is especially sensitive to higher-frequency anomalies. Hence, relating a set of regional-scale gravity observations to the radial Laplacian component given by (18) can be useful for studying the shallower crustal anomaly components of the data. Also, the zero contour of equation (18) can be used to roughly delineate the lateral extent of the anomaly source because the edges of the source are approximated by the inflection points of the anomaly which correspond to zero curvature. From the sign convention used in equation (18) it is obvious that the zero contour which delineates regions of positive or negative radial Laplacian values outlines, respectively, regions of positively or negatively contrasting densities.

In consideration of the foregoing derivations it is clear that the results of this section are linearly related by geometry through equation (3). Hence, once a set of gravity observations has been suitably related to a distribution of point poles according to equation (8), then all the variables necessary for evaluating the gravitational potential, anomaly vector components and spatial derivatives, as well as the continuation of any of these quantities, also have been determined for the observation set.

3. The magnetic point dipole potential

The magnetic point dipole is defined as a dipole of negligible length when compared to the distance between the dipolar source and observation points. Its scalar magnetic potential $MP(R)$ evaluated at the observation point (r, θ, ϕ) located a distance $\vec{R}$ from the source point (r_1, θ_1, ϕ_1) is given by:

$$MP(R) = \Delta\vec{j} \cdot \vec{\nabla}_1\left(\frac{1}{R}\right) = -\Delta\vec{j} \cdot \vec{\nabla}\left(\frac{1}{R}\right) \qquad (20)$$

where $\vec{\nabla}_1$ = the gradient operator in source point coordinates such that $\vec{\nabla}_1(1/R) = -\vec{\nabla}(1/R)$ in observation point coordinates, R = given in (2), and $\Delta\vec{j}$ = the magnetic polarization contrast vector of the source point. The relationships between source point and observation point geometry are illustrated in Fig. 1.

As shown in Fig. 2, the polarization contrast vector may be expressed in terms of its inclination, I_1, and declination, D_1, and the spherically orthonormal basis vectors of the source point as:

$$\Delta\vec{j} = \Delta j * \vec{u}_1 = \Delta j * \{(\sin I_1)\,\hat{e}_r + (\cos I_1 \cos D_1)\,\hat{e}_\theta + (\cos I_1 \sin D_1)\,\hat{e}_\phi\} \qquad (21)$$

where $\vec{u}$ = the unit polarization field vector. Here, it should be noted that if polarization is induced only, then the polarization contrast is given by:

$$\Delta\vec{j} = \Delta k * \vec{F}_1 \qquad (22)$$

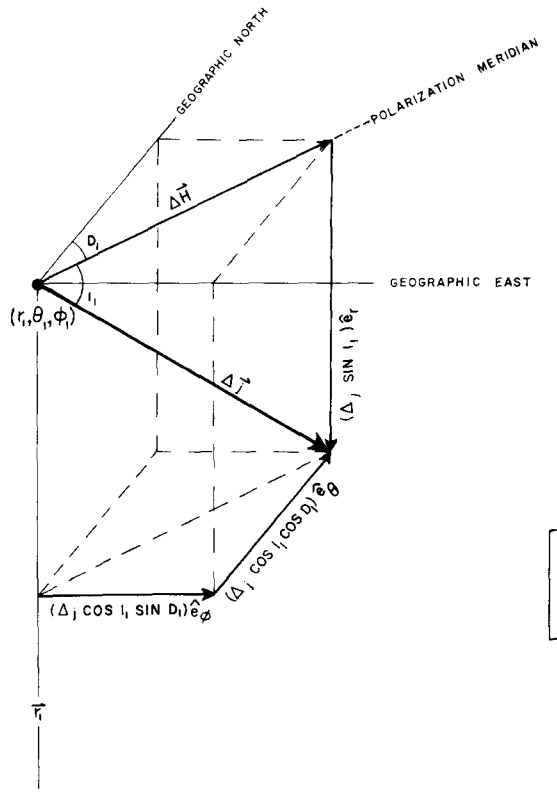

SCALAR MAGNETIC POLARIZATION ELEMENTS

$\Delta H = \Delta_j \cos I_1$	(HORIZONTAL COMPONENT)
$\Delta_j(r_1) = \Delta_j \sin I_1$	(RADIAL COMPONENT)
$= \Delta H \tan I_1$	
$\Delta_j(\Theta_1) = \Delta H \cos D_1$	(LATITUDE COMPONENT)
$\Delta_j(\Phi_1) = \Delta H \sin D_1$	(LONGITUDE COMPONENT)
$\Delta H^2 = \Delta_j(\Theta_1)^2 + \Delta_j(\Phi_1)^2$	
$\Delta_j{}^2 = \Delta_j(\Theta_1)^2 + \Delta_j(\Phi_1)^2 + \Delta_j(r_1)^2$	
$= \Delta H^2 + \Delta_j(r_1)^2$	

MAGNETIC POLARIZATION VECTOR

$$\Delta\vec{j} = \Delta_j\vec{u}_1 = \Delta_j\left[(\sin I_1)\hat{e}_r + (\cos I_1 \cos D_1)\hat{e}_\theta + (\cos I_1 \sin D_1)\hat{e}_\phi\right]$$
$$= \Delta\vec{j}(r_1) + \Delta\vec{j}(\theta_1) + \Delta\vec{j}(\phi_1)$$

Fig. 2. Geometry of the magnetic polarization contrast vector, $\Delta\vec{j}$, at the point (r_1, θ_1, ϕ_1) in terms of the orthonormal spherical basis vectors, $\hat{e}_r$, $\hat{e}_\theta$, and $\hat{e}_\phi$. In the absence of remanence, the polarization of the point dipole at (r_1, θ_1, ϕ_1) is induced only and $\Delta\vec{j} = \Delta k * \vec{F}_1$, where Δk = volume magnetic susceptibility and $\vec{F}_1$ is the geomagnetic field vector with inclination and declination I_1 and D_1, respectively.

where Δk = the magnetic susceptibility contrast, and $\vec{F}_1$ = the geomagnetic field vector at the source point such that $\vec{F}_1 = F_1 * \vec{u}_1$.

According to equations (21) and (4), (5) and (6) the magnetic scalar potential of a point dipole reduces to:

$$MP(R) = -\Delta\vec{j} \cdot \vec{\nabla}\left(\frac{1}{R}\right) = \left\{-\vec{u}_1 \cdot \vec{\nabla}\left(\frac{1}{R}\right)\right\}\Delta j$$

$$= \left\{-\frac{\partial}{\partial R}\left(\frac{1}{R}\right) * \vec{u}_1 \cdot \vec{\nabla}R\right\}\Delta j$$

$$= \frac{\Delta j}{R^2} * \left\{\sin I_1\left(\frac{\partial R}{\partial r}\right) + \cos I_1 \cos D_1\left(\frac{1}{r}\frac{\partial R}{\partial \theta}\right)\right.$$

$$\left. + \cos I_1 \sin D_1\left(\frac{1}{r \sin\theta}\frac{\partial R}{\partial \phi}\right)\right\}$$

$$= \frac{\Delta j}{R^3} * \{\sin I_1(A) + \cos I_1 \cos D_1(B)$$

$$+ \cos I_1 \sin D_1(C)\}$$

$$= \frac{\Delta j}{R^3} * E \qquad (23)$$

Now, the vector magnetic force field, $MF(\vec{R})$, at distance $\vec{R}$ due to the point dipole scalar potential is given by:

$$MF(\vec{R}) = -\vec{\nabla}\{MP(R)\}$$

$$= -\left\{\vec{\nabla}\left(\frac{1}{R^3}\right) * E + \frac{1}{R^3} * \vec{\nabla}E\right\}\Delta j$$

$$= -\left\{\frac{\partial}{\partial R}\left(\frac{1}{R^3}\right)\vec{\nabla}R * E + \frac{1}{R^3}\left(\frac{\partial E}{\partial R}\right)\vec{\nabla}R\right\}\Delta j$$

$$= MF(r)\,\hat{e}_r + MF(\theta)\,\hat{e}_\theta + MF(\phi)\,\hat{e}_\phi \qquad (24)$$

where:

$$MF(r) = \left\{\frac{-A}{R^4} * J\right\}\Delta j, \quad MF(\theta) = \left\{\frac{-B}{R^4} * J\right\}\Delta j,$$

$$MF(\phi) = \left\{\frac{-C}{R^4} * J\right\}\Delta j,$$

and:

$$J = \left(\frac{R}{A} - \frac{3A}{R}\right)\sin I_1 + \left(\frac{Rr_1\cos\delta}{B} - \frac{3B}{R}\right)\cos I_1 \cos D_1$$

$$+ \left(\frac{Rr_1 \sin\theta_1 \cos(\phi - \phi_1)}{C} - \frac{3C}{R}\right)\cos I_1 \sin D_1$$

Equation (24) is useful for representing vector magnetic anomaly data. However, most magnetic data taken for geophysical applications represent scalar total anomaly intensity measurements which contain no information to discriminate the vector components. For geophysical interpretation, then, the assumption is made that the magnetic anomaly due to geological magnetization variations is so small that perturbations of the geomagnetic field in any direction other than its direction are negligible. Kontis and Young [9] have shown this assumption to be reasonably valid for anomalies with amplitudes less than about 10,000 gammas * in the earth's magnetic field. Hence, for geophysical interpretation purposes, a total magnetic anomaly measurement is taken to represent a perturbation of the geomagnetic field along its direction at the point of measurement.

Thus, to represent a set of total intensity measurements in terms of the magnetic field of point dipoles it is necessary to compute equation (24) in the direction of the geomagnetic field at the observation points. This can be achieved by taking the vector dot product between equation (24) and the unit geomagnetic field vector, $\vec{u}$, at the observation point. Accordingly, the total magnetic anomaly, ΔT, at $\vec{R}$ due to the point dipole is:

$$\Delta T = \vec{u} \cdot MF(\vec{R}) = \left[-\vec{u} \cdot \vec{\nabla}\left(\vec{u}_1 \cdot \vec{\nabla}_1\left(\frac{1}{R}\right)\right)\right]\Delta j$$

$$= MF(r)\sin I + MF(\theta)\cos I \cos D$$

$$+ MF(\phi)\cos I \sin D \qquad (25)$$

* 1 gamma = 1 nanoTesla, nT.

where I and D are the inclination and declination, respectively, of the geomagnetic field at the observation point. In the application of equation (25) geomagnetic field models such as the IGRF-1965 [10] commonly are used to obtain pertinent values of (I_1, D_1, F_1) at the source point and (I, D) at the observation point.

Consideration of equation (25) in its expanded form suggests that the derivation of derivatives for total anomaly fields is likely to yield fairly complicated algebraic expressions. Fortunately, these expressions can be considerably simplified by reducing the data to the pole which in effect is an adjustment of the anomalies to what they would be if radially (vertically) polarized by a magnetic field of uniform intensity. In conventional applications the spatial scale of the magnetic survey is small enough that a single value of geomagnetic field inclination, declination and amplitude may be assumed for the pole reduction. Over regional-scale areas, however, magnetic anomalies must be differentially reduced to the pole for values of geomagnetic inclination, declination and amplitude which are variable at all source and observation point locations.

For total magnetic anomaly observations referenced to a distribution of equivalent point dipoles according to equation (25), differential reduction to radial polarization is readily achieved by setting $I = I_1 = 90°$, $D = D_1 = 0°$ and using the normalized polarization $\Delta j'$ given by $\Delta j' = \Delta j(N/F_1)$ where N is the desired polarizing amplitude. Accordingly, equation (25) reduced to the pole leads to a considerably simplified radial polarization anomaly $\Delta T(N)$ given by:

$$\Delta T(N) = -\left\{\frac{1}{R^3} - \frac{3A^2}{R^5}\right\}\Delta j' \qquad (26)$$

An assumption which is implicit in the application of (26) is, of course, that the magnetic anomalies contain no appreciable component of remanence. When this condition holds, equation (26) can be used to adjust the magnetic observations so that they uniformly reflect anomaly source characteristics of geometry and magnetization. Because of this considerable practical significance to geophysical interpretation, the radially polarized anomaly, $\Delta T(N)$, in general is more suitable for derivative analysis that the total field anomaly, ΔT.

The first-order spatial derivatives of a set of verti-

cally polarized magnetic anomalies may be obtained from the negative gradient of (26) which is:

$$-\vec{\nabla}\{\Delta T(N)\} = \vec{\nabla}\left\{\frac{1}{R^3} - \frac{3A^2}{R^5}\right\}\Delta j'$$

$$= \vec{\nabla}R\left\{\frac{9}{R^4} - \frac{15A^2}{R^6}\right\}\Delta j'$$

where the scalar first radial derivative of $\Delta T(N)$ is given by:

$$-\frac{\partial \Delta T(N)}{\partial r} = \left\{\frac{15A^3}{R^7} - \frac{9A}{R^5}\right\}\Delta j' \tag{27}$$

the scalar first horizontal θ-gradient component of $\Delta T(N)$ is:

$$-\frac{1}{r}\frac{\partial \Delta T(N)}{\partial \theta} = \left\{\frac{15A^2B}{R^7} - \frac{9B}{R^5}\right\}\Delta j' \tag{28}$$

and the scalar first horizontal ϕ-gradient component of $\Delta T(N)$ is:

$$-\frac{1}{r\sin\theta}\frac{\partial \Delta T(N)}{\partial \phi} = \left\{\frac{15A^2C}{R^7} - \frac{9C}{R^5}\right\}\Delta j' \tag{29}$$

Also, because $\Delta T(N)$ is a potential function its Laplacian is zero, so that the radial Laplacian component of $\Delta T(N)$ may be equated with the horizontal component according to the relation:

$$-\left\{\frac{\partial^2 \Delta T(N)}{\partial r^2} + \frac{1}{r}\frac{\partial \Delta T(N)}{\partial r}\right\}$$

$$= \frac{1}{r^2}\left\{\frac{\partial^2 \Delta T(N)}{\partial \theta^2} + \cot\theta\,\frac{\partial \Delta T(N)}{\partial \theta} + \frac{1}{\sin^2\theta}\frac{\partial^2 \Delta T(N)}{\partial \phi^2}\right\} \tag{30}$$

where the second derivative of $\Delta T(N)$ is given by:

$$\frac{\partial^2 \Delta T(N)}{\partial r^2} = \left\{\frac{109A^4}{R^9} - \frac{90A^2}{R^7} + \frac{9}{R^5}\right\}\Delta j' \tag{31}$$

4. Combined gravity and magnetic point source potentials

For a point mass which also is magnetized, the observation-to-source point geometry is invariant so that the magnetic and gravitational potentials of the point source can be compared directly. Consideration of equations (14) and (26), for example, shows that for a common point source the gravity effect and radially polarized magnetic anomaly are related by:

$$\Delta T(N) = \frac{\Delta j'}{G * \Delta m} * \frac{\partial \Delta g}{\partial r}$$

$$= \frac{\Delta j'}{G * \Delta m} * \Delta g\left\{\frac{1}{A} - \frac{3A}{R^2}\right\} \tag{32}$$

When the magnetic anomaly is calculated directly from the gravity potential as in equation (32), the result commonly is called the pseudo-magnetic anomaly. The corresponding pseudo-gravity anomaly, on the other hand, is given by:

$$\Delta g = \frac{G * \Delta m}{\Delta j'} * \Delta T(N)\left\{\frac{A * R^2}{R^2 - 3A^2}\right\} \tag{33}$$

Pseudo-potential field calculations facilitate enhanced geologic interpretation of gravity and magnetic anomalies. The procedure, for example, is to relate an observed gravity anomaly to a set of point masses, Δm, by least squares matrix inversion as described in the next section. Comparing an estimate for the bulk magnetization contrast-to-density contrast ratio of the anomalous body to the equivalent point masses, Δm, gives corresponding equivalent point magnetizations, $\Delta j'$, which can be used to calculate the pseudo-magnetic anomaly from equation (32) or, even more simply, from equation (26). A similar procedure can be used to develop from an observed magnetic anomaly the corresponding pseudo-gravity anomaly using equations (33) or (8). If the pseudo-potential field anomalies are similar to the observed potential field anomalies, common source structure can be inferred for both magnetic and gravity anomalies, thus, minimizing the ambiguity inherent to the analysis of each of the anomalies by itself. Of course, dissimilarity between pseudo and observed anomalies also can lead to valid inferences regarding source lithology and structure.

Equations (32) and (33) are special consequences of a more general result known as Poisson's theorem [11] which describes the relationship between the gravitational and magnetic potentials of any uniformly dense and magnetized body. In its geophysical context Poisson's theorem states that at an observa-

tion point the resultant magnetic anomaly is related to the first derivative of the gravity anomaly taken in the direction of magnetization by the magnetization contrast-to-density contrast ratio of the body. By equation (3) it is clear that Poisson's theorem also can be extended to relate the nth magnetic anomaly derivative to the appropriate $(n + 1)$th gravity anomaly derivative. Equations (19) and (27), for example, combine to relate the second-order radial gravity anomaly derivative to the radially polarized first-order magnetic anomaly derivative for a common point source. In general, then, Poisson's theorem provides an important quantitative basis for comparing gravity and magnetic anomalies and, hence, for minimizing the ambiguity associated with the lithologic interpretation of these potential fields.

5. The inversion problem

As described previously, the measured potential field anomaly at any observation point is the summation at the observation point of the potential field effects due to each of the anomalous sources. Because of source ambiguity of potential fields it is clear that distributions of point sources exist for any measured anomaly such that the integrated anomalous effect of the point sources represents with equivalent facility the observed integrated effect of the true sources. The current objective, then, is directed toward resolving the problem of obtaining for a given set of observed potential field anomalies, a distribution of equivalent point sources suitable for processing purposes.

The effort begins from a consideration of equations (8) and (25) which relate equivalent point sources to measured anomalies of the earth's radial gravity field or total magnetic intensity field, respectively. Both of these equations may be generalized as shown in Fig. 1, so that the incremental anomaly effect due to the pth point source at the nth observation point is given by $q_{np}(R) * \Delta x_p$, where $q_{np}(R)$ is the geometric point source function and Δx_p is the appropriate physical property value. Accordingly, the relationship between a set of n observations (obs_1, obs_2, ..., obs_n) and a set of p point sources can be expressed by the system of linear equations:

$$q_{11} * \Delta x_1 + q_{12} * \Delta x_2 + \ldots + q_{1p} * \Delta x_p = obs_1$$

$$q_{21} * \Delta x_1 + q_{22} * \Delta x_2 + \ldots + q_{2p} * \Delta x_p = obs_2$$

$$\vdots \qquad \vdots \qquad \vdots \qquad \vdots$$

$$q_{n1} * \Delta x_1 + q_{n2} * \Delta x_2 + \ldots + q_{np} * \Delta x_p = obs_n$$

In matrix notation the linear system is more conveniently described by:

$$Q * \Delta X = \mathrm{OBS} \tag{34}$$

where Q is an (n-row by p-column) matrix with elements given by the geometric point source functions $[q_{np}(R)]$, ΔX is a (p by 1) column matrix containing the physical property values (Δx_p), and OBS is an (n by 1) column matrix of the anomaly observations (obs_n).

Now, the geometric variables of the observation points are known, so that the complete determination of the elements of Q can be made by simply specifying the geometric distribution of the equivalent point sources. Hence, by pre-determining the equivalent point source locations equation (34) can be solved for a set of physical property values ΔX by a number of well known matrix inversion techniques.

For example, when $p = n$, Q is a square matrix and the exact solution given by:

$$\Delta X = Q^{-1} * \mathrm{OBS} \tag{35}$$

can be obtained by well documented numerical methods (e.g. [12]), if Q is not near-singular. Because the number of anomaly observations considered in most applications is large, it generally is more efficient to set up problem (34) so that the number (p) of equivalent point sources is substantially less than the number (n) of observations.

When $p < n$, the solution to the overconstrained system of equation (34) is given by:

$$\Delta X = (Q^{\mathrm{T}}Q)^{-1} * Q^{\mathrm{T}} * \mathrm{OBS} \tag{36}$$

This solution is well known in the literature of numerical methods as a least squares solution in the sense that it minimizes the Euclidean vector norm of the residual, $|\mathrm{OBS} - Q * \Delta X|^2$. Assuming the problem is properly scaled so that Q is not near-singular, procedures for obtaining (36) fall generally into two

basic categories depending on how the values of the solution vector are to be used in subsequent analysis.

For processing purposes such as continuation, differentiation, etc., the solution ΔX merely represents a set of weighting coefficients which operate on suitably modified geometric point source functions to achieve a least squares approximation of the processed observations. The physical reality of the property values contained in ΔX are of limited consequence to these processing objectives and all that is required, simply, is a set of property values which provide a least squares fit between the observed anomalies and equivalent point source anomalies. To obtain this type of solution, numerous methods are available for application (e.g. [13,14]).

The second major solution category occurs when it is desired to constrain the values of the solution vector ΔX for subsequent analysis. This situation arises, for example, when physically realistic property values are required for modeling volume elements of the crust or some other geologic feature of the earth. Constrained solutions to equation (34) can be achieved by the eigenvalue-eigenvector matrix decomposition analysis suggested by Lanczos [15].

Accordingly, the eigenvalue-eigenvector decomposition of Q is given by $Q = U * S * V^{T}$ to yield the solution vector:

$$\Delta X = (V * S^{-1} * U^{T}) * \mathrm{OBS} \qquad (37)$$

Here, U and V are orthogonal matrices with columns which are the eigenvectors associated with the columns and rows of Q, respectively, and S is a diagonal matrix with elements which are the eigenvalues, λ, of Q. The eigenvalues and eigenvectors are obtained from the square symmetric product matrix $Q^{T}Q$ and the inverse S^{-1} is a diagonal matrix of eigenvalue inverses, $1/\lambda$. Jackson [16] has shown that the Lanczos solution (37) is a least squares solution for the overconstrained system (i.e., $p < n$) and, hence, is identical to the conventional solution (36) when Q is not near-singular. Efficient procedures for obtaining eigensystem solutions also are available in the general literature for application (e.g. [17]).

Finally, the problem of specifying the geometric distribution of equivalent point sources for purposes of efficient inversion must be considered. In practice, machine computation time and storage requirements frequently dictate the source distribution characteristics for inversion. As discussed by Bowman et al. [18], these requirements can be minimized by the strategic assignment of a point source to each feature of the observed data that is to be modeled. Here, the geometric characteristics of the strategi :e distribution can be specified according to well known rules relating the depth and wavelength characteristics of point sources (e.g. [19,20]).

Another numerically convenient approach which is more automatic in its application, is to perform the inversion on a spherical grid of point sources at constant depth. For this application, the initial depth of the source grid should be on the order of the source grid spacing (e.g. [6,21]). In practice, the source grid density of unknowns generally is specified according to available computer resources, so that adjustments of the equivalent source field to more presicely reflect wavelength characteristics of the observed data normally reduce to straightforward adjustments of the source grid depth.

It also should be noted that edge effects frequently are observed in radial continuations of the equivalent source field when the lateral dimensions of the source grid are roughly coincident with the observation grid. This result reflects the decreased energy density associated with point sources located near the edges of the distribution that tends to be emphasized by continuation. Edge effects are particularly troublesome when the observed data set is so large that processing has to be accomplished via subsets at one elevation which must be rejoined at a new elevation. Experience has shown, however, that edge effects can be minimized by including in the inversion a peripheral rind of observed data which extends laterally beyond the source grid a distance roughly equal to or greater than the radial distance between the source grid and the desired elevation of continuation.

6. Examples of geophysical processing applications

To illustrate the equivalent point source inversion technique and its processing capabilities, regional gravity and magnetic anomaly data obtained from NASA-GSFC for the United States, Mexico and Central America are considered. Accordingly, Fig. 3A

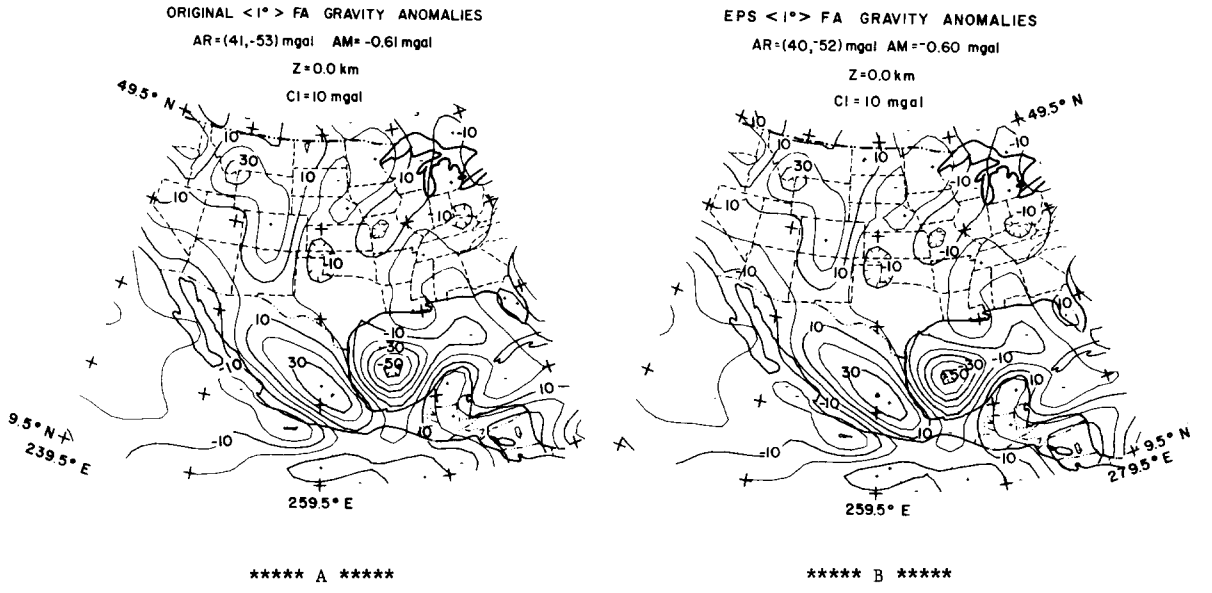

Fig. 3. A. Stereographic equal-area polar (SEAP) projection of smoothed 1°-averaged free-air gravity anomaly data for the United States, Mexico and Central America. Amplitude range (*AR*) of the data set is 41 to −53 mgal and the amplitude mean (*AM*) is −0.61 mgal. Contour interval (*CI*) is 10 mgal and the reference elevation (*Z*) of the observations is 0.0 km. B. Equivalent point source (EPS) approximation of smoothed 1°-averaged free-air gravity anomalies.

shows a stereographic equal-area polar (SEAP) projection * of smoothed 1°-averaged free-air gravity anomalies observed for the region 239.5–280.5°E longitude and 9.5–50.5°N latitude. The observation grid consists of (42,42)-values at 1° spacing where the relative elevation (*Z*) of the observations is 0.0 km. The amplitude range (AR) of the observations is between 41 and −53 mgal and the amplitude mean (AM) is −0.61 mgal.

The least squares representation of the observations by equivalent point source inversion is given in Fig. 3B. Here, the observations are inverted on a source grid of (15,15)-values to obtain the least squares solution vector of density contrasts given by equation (36). The point source grid spans the region 240–280°E, 10–50°N at a depth of 400 km below the relative elevation of the observation grid. The point sources are uniformly spaced at 2.857° intervals over the source grid. As shown by a consideration of the amplitude means of Fig. 3A and B, the mean error of the least squares fit of the observed gravity data is negligible.

An obvious by-product of the inversion is a least squares density model for the observed gravity anomalies. By Brun's formula [23], if the anomalous potential of the model is known, then the geoid height anomaly due to the anomalous mass is given by the ratio of anomalous potential to normal gravity (= 9.8 m/s^2). A least squares estimate of the gravitational potential of the observed anomalies can be readily computed by integrating at each observation point the potentials due to each of the source points according to equation (1). Hence, by dividing this result by the normal acceleration of gravity a least squares approximation of the geoidal anomalies can be obtained. Accordingly, Fig. 4A illustrates a least squares representation of the geoidal deflections due to the mass anomalies responsible for the observed free-air gravity anomaly data of Fig. 3A. The geoidal deflections given in Fig. 4A are accurate on a relative basis. However, when compared to global-scale geoids, these anomalies must be adjusted by a nearly constant value that reflects the broad-scale geoidal deflection due to long-wavelength variations of the

* This mapping is a Lambert azimuthal equal-area projection [22] referenced to either of the geographic poles depending upon the hemisphere being considered.

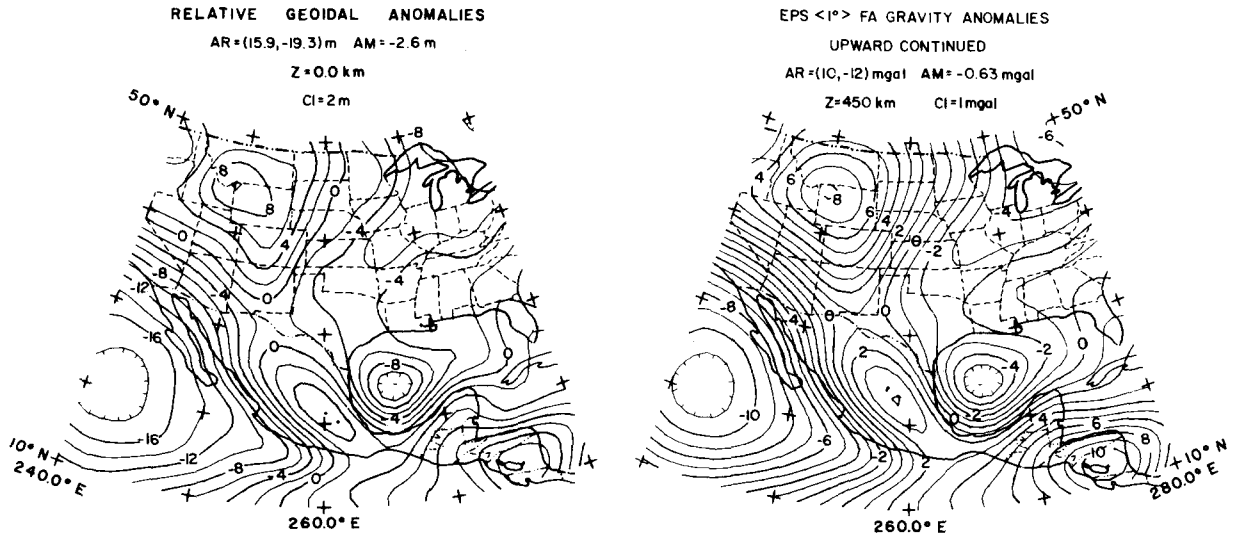

Fig. 4. A. Relative geoidal anomalies derived from equivalent point source inversion of smoothed 1°-averaged free-air gravity anomalies. B. Equivalent point source approximation of smoothed 1°-averaged free-air gravity anomalies upward continued to 450 km elevation.

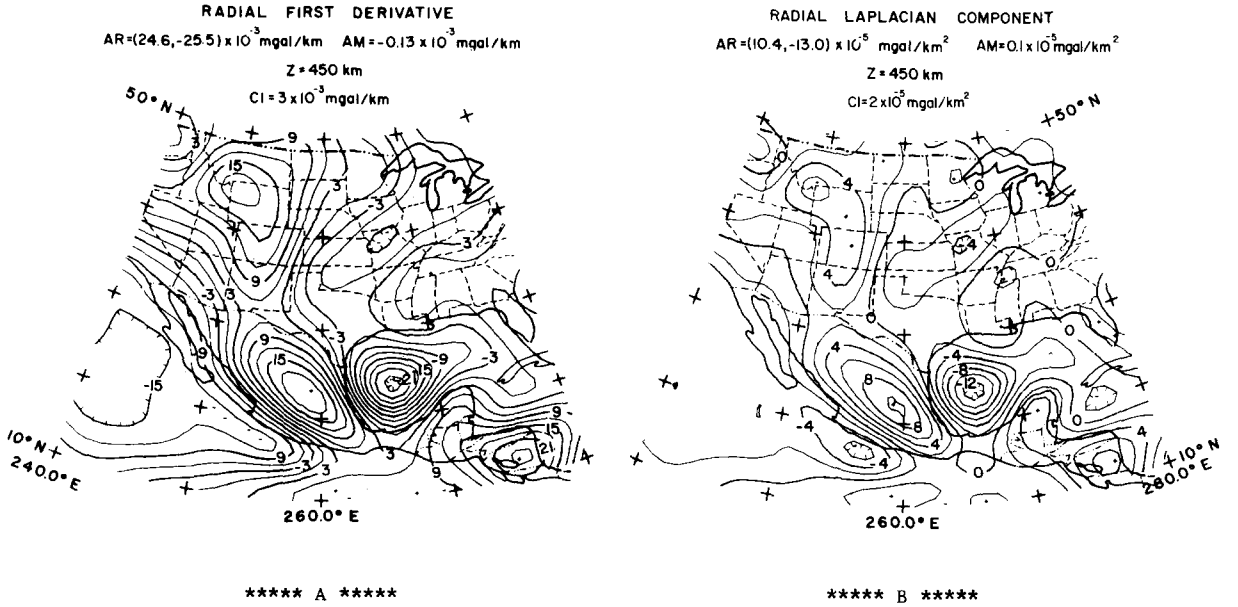

Fig. 5. A. Equivalent point source approximation of the first radial derivative of smoothed 1°-averaged free-air gravity anomalies. B. Equivalent point source approximation of the radial Laplacian component of smoothed 1°-averaged free-air gravity anomalies. At 450 km elevation, the radial Laplacian component is nearly identical to the second radial derivative of the gravity anomalies.

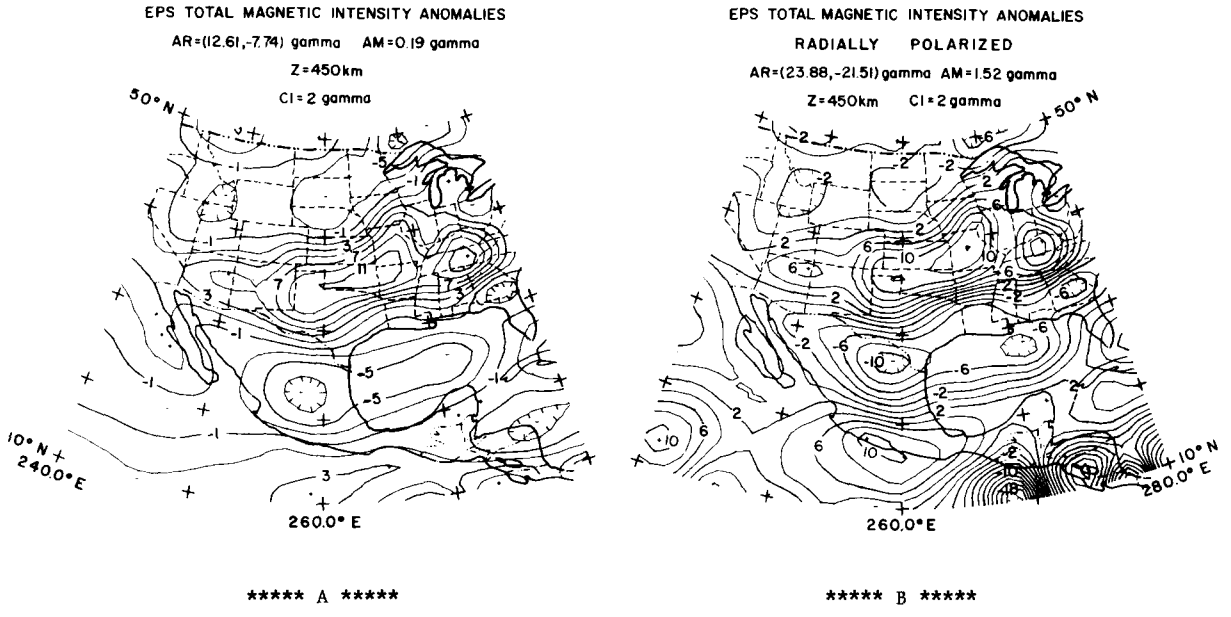

Fig. 6. A. Multielevation POGO satellite magnetometer data reduced to a common elevation of 450 km by equivalent prism source inversion according to the procedures of Mayhew [8]. B. Equivalent source approximation of the total magnetic intensity anomaly data differentially reduced to the radial pole. The normalization amplitude (N) assumed for the radially polarizing field was 60,000 gammas.

gravitational potential which are too large to be adequately sampled by the restricted spatial coverage considered in this illustration.

Another processing example is given in Fig. 4B where the results of the inversion are used to obtain a least squares representation of the observed gravity anomalies upward continued to a typical satellite elevation. In this application, the gravity effect of the equivalent point sources was recomputed at 450 km elevation using equation (8). Further processing applications are shown in Fig. 5A and 5B where the inversion results are used to obtain least squares representations at 450 km elevation of the radial first derivative and Laplacian component of the observed gravity data according to equations (14) and (18), respectively. At 450 km elevation, it turns out that the radial Laplacian is nearly identical to the second radial derivative field of the gravity anomalies. Note also, that the anomalies given in Figs. 4A, B and 5A , B all have now been reregistered to integral degree nodes of the spherical grid spanning the region 240–280°E, 10–50°N at 1°-station intervals.

In Fig. 6A, an equivalent source dipole field representation of POGO satellite magnetometer observations conducted during 1968 is presented. The magnetic data were reduced in profile form according to the procedures described by Mayhew [8] to yield 4271 anomaly values from 345 satellite tracks ranging in elevation between 240 km and 700 km over the study area. To reduce the total magnetic anomalies to a common elevation the profile data were inverted on a spherical grid of (15,15) spherical prisms * to obtain the least squares solution vector of dipole moments given in (36). The equivalent prism source grid was located at the surface of the earth and uniformly spanned the region 240–280°E, 10–50°N at 2.857° intervals. The dipoles were oriented along the main geomagnetic field directions given by the IGRF-1965 updated to 1968. The fit of the equivalent source field to the observed profile data is to 1 gamma standard deviation. Examples illustrating the general degree

* To convert the spherical prismatic dipolar moment formulation of Mayhew [8] to point dipole moments, it is necessary only to multiply the prismatic moments by the spherical volumes of the corresponding prisms.

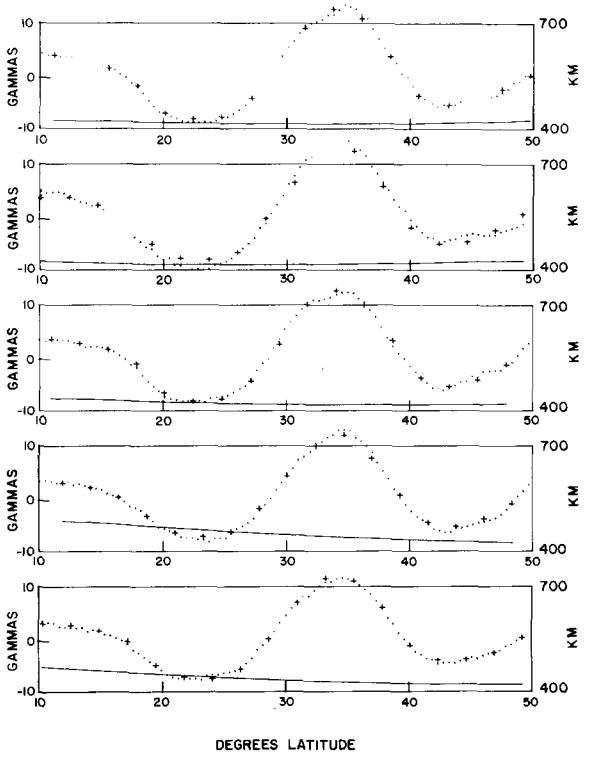

Fig. 7. Total magnetic intensity anomaly comparisons (after Mayhew [8]) illustrating the fit between arbitrarily selected tracks of POGO satellite magnetic measurements (dots) and the corresponding equivalent source values (crosses). The solid line in each comparison corresponds to the elevation of the POGO satellite magnetometer data.

of this fit for an arbitrary selection of profiles between 10°N and 50°N are given in Fig. 7. Recomputing the equivalent source field at 450 km elevation using equation (25) modified to include spherical prismatic volumes gives the least squares representation shown in Fig. 6A of variable elevation satellite magnetic anomaly data reduced to a common elevation of 450 km.

Assuming that the magnetization is predominantly by induction, the variable influence of the geomagnetic field on the total magnetic intensity anomalies recorded in Fig. 6A can be eliminated by differentially reducing the data to vertical polarization. This result is achieved by recomputing the equivalent source field using equation (26) modified for spherical prisms. Accordingly, Fig. 6B illustrates the least squares representation of the total magnetic anomaly data of Fig. 6A differentially reduced to the pole using a normalized polarizing amplitude (N) of 60,000 gammas.

A comparison of Fig. 6A and 6B shows that anomalies in the southern portion of the radially polarized map generally are shifted differentially from 3° to as much as 5° to the north. Larger amplitudes also are observed for these anomalies because of the positive difference between the scalar intensities of the radially polarizing field and the IGRF-1965 updated to 1968 at low latitudes. Northern amplitudes, on the other hand, show only slight relative alterations which include principally northward displacements that rarely exceed 1° or 2°. The behavior of the radially polarized data, then, is consistent with that anticipated for the conventional pole reduction.

In consideration of the foregoing examples it is clear that once a set of potential field anomalies have been related to a set of equivalent point sources by least squares matrix inversion, then a number of geophysically interesting characteristics of the observed data also are known with equivalent least squares precision. In general, these characteristics include the associated potentials, vector anomaly components and spatial derivatives, as well as continuations of these elements.

7. Conclusions

Equivalent point source inversion is an efficient and versatile approach to spherical earth processing of regional potential field anomalies. The procedure is to relate observed anomalies to a set of equivalent point sources by a system of linear equations. By predetermining the locations of the point sources, the problem simplifies to solving the linear equation system for a solution vector of physical property values. In practice, the system of equations normally is overconstrained in the sense that the number of point source physical property values of the solution is less than the number of observed anomaly values. From the general literature of numerical methods, however, several well-known matrix inversion methods are available to obtain the solution vector such that the resultant equivalent source field is a least squares representation of the observed data.

The anomalous potential and its spatial derivatives of all orders are linearly related so that when an equiv-

alent point source least squares representation for any one of these elements has been determined, representations with equivalent least squares precision also are available for the rest of the elements by simple linear transformations. This result has great practical significance because considerable geophysical information is related to the anomalous potential and its spatial derivatives. From the least squares inversion of observed gravity anomalies, for example, geoidal anomalies, vector anomaly components and derivatives at any point in source-free space also may be computed with equivalent least squares precision. Similarly, the results of equivalent point source inversion of observed magnetic anomalies can be used to obtain least squares representations at any point in source-free space of the vector anomaly components, differential pole reductions and spatial derivatives. Pseudo-potential field calculations also can be readily performed using the equivalent point source inversion formulation.

In consideration of these results, it is concluded that equivalent point source inversion represents a powerful and efficient method for spherical earth processing of regional-scale gravity and magnetic anomalies. Accordingly, the method has widespread application in the analysis and design of regional-scale gravity and magnetic surveys for lithospheric investigation.

Acknowledgements

Financial support for this investigation was provided by the Goddard Space Flight Center under NASA contracts NAS5-22816 and NAS5-25030.

References

1 W.M. Kaula, Theory of statistical analysis of data distributed over a sphere, Rev. Geophys. 5 (1967) 83–107.
2 G.P. Woollard, The relationship of gravity anomalies to surface elevation, crustal structure and geology, Univ. Wisc. Geophys. Polar Res. Center, Res. Rep. SER. 62-9 (1962).
3 W.E. Strange and G.P. Woollard, The use of geologic and geophysical parameters in the evaluation, interpolation and prediction of gravity, Hawaii Inst. Geophys. Doc. HIG-64-17 (1964).
4 A.S. Ramsey, An Introduction to the Theory of Newtonian Attraction (Cambridge University Press, New York, N.Y., 1940).
5 O.D. Kellog, Foundations of Potential Theory (Dover Publications, New York, N.Y., 1953).
6 C.N.G. Dampney, The equivalent source technique, Geophysics 34 (1969) 39–53.
7 D.A. Emilia, Equivalent sources used as an analytical base for processing total magnetic field profiles, Geophysics 38 (1973) 339–348.
8 M.A. Mayhew, Inversion of satellite magnetic anomaly data, J. Geophys. 45 (1979) 119–128.
9 A.L. Kontis and G.A. Young, Approximation of redisual total-magnetic intensity anomalies, Geophysics 29 (1964) 623–627.
10 J.C. Cain, S.J. Hendricks, R.A. Langel and W.V. Hudson, A proposed model for the International Geomagnetic Reference Field-1965, J. Geomag. Geoelectr. 19 (1967) 335–355.
11 S.D. Poisson, Mémoire sur la théorie du magnétisme, Mém. Acad. R. Sci. Inst. Fr. (1826) 247–348.
12 B. Carnahan, H.A. Luther and J.O. Wilkes, Applied Numerical Methods (Wiley, New York, N.Y., 1969).
13 C.L. Lawson and R.J. Hanson, Solving Least Squares Problems (Prentice-Hall, Princeton, N.J., 1974).
14 J.J. Dongarra, F.R. Bunch, C.B. Moler and G.W. Stewart, LINPACK User's Guide (SIAM, Philadelphia, Pa., 1979).
15 C. Lanczos, Linear Differential Operators (D. Van Nostrans, London, 1961).
16 D.D. Jackson, Interpretation of inaccurate, insufficient and inconsistent data, Geophys. J.R. Astron. Soc. 28 (1972) 97–109.
17 B.T. Smith, J.M. Boyle, B.S. Garbow, Y. Ikebe, V.C. Klema and C.B. Moler, Matrix Eigensystem Routines – EISPACK Guide, Lecture Notes in Computer Science, 6 (Springer, Stuttgart, 1976).
18 P.L. Bowman, L.W. Braile, V.W. Chandler, W.J. Hinze, A.J. Luca amd R.R.B. von Frese, Magnetic and gravity anomaly correlation and its application to satellite data, NASA-GSFC TM79702 (1979).
19 L.L. Nettleton, Gravity and magnetic calculations, Geophysics 7 (1942) 293–310.
20 D.W. Smellie, Elementary approximations in aeromagnetic interpretation, Geophysics 21 (1956) 1021–1040.
21 C.C. Ku, A direct computation of gravity and magnetic anomalies caused by 2- and 3-dimensional bodies of arbitrary shape and arbitrary magnetic polarization by equivalent point method and a simplified cubic spline, Geophysics 42 (1977) 610–622.
22 E.C. Kalkani and R.R.B. von Frese, An efficient construction of equal-area fabric diagrams, Comput. Geosci. 5 (1979) 301–311.
23 W.A. Heiskanen and H. Moritz, Physical Geodesy (W.J. Freeman, San Francisco, Calif., 1967).